

# Away-from-jet energy flow\*

---

**A. Banfi, G. Marchesini, G. Smye**

*Dipartimento di Fisica, Università di Milano-Bicocca and  
INFN, Sezione di Milano, Italy*

**ABSTRACT:** We consider interjet observables in hard QCD processes given by the energy flow  $E_{\text{out}}$  in a region away from all hard jets. Here the QCD radiation is depleted ( $E_{\text{out}} \ll Q$ ), and therefore these observables provide ideal means to study non-perturbative effects. We derive an evolution equation (in the large  $N_c$  limit) which resums, for large  $Q/E_{\text{out}}$ , all leading terms arising from large angle soft emission (double logarithms are absent). We discuss the analytical features of the result and identify universal and geometry-dependent contributions. Our analysis confirms features found using numerical methods by Dasgupta and Salam.

**KEYWORDS:** QCD, Jets, LEP HERA and SLC Physics, Hadronic Colliders.

---

\*Research supported in part by the EU Fourth Framework Programme, ‘Training and Mobility of Researchers’, Network ‘Quantum Chromodynamics and the Deep Structure of Elementary Particles’, contract FMRX-CT98-0194 (DG12 - MIHT).

---

## Contents

<b>1. Introduction</b>	<b>1</b>
<b>2. The observable</b>	<b>3</b>
<b>3. QCD resummation</b>	<b>4</b>
<b>4. Evolution equation</b>	<b>5</b>
4.1 Comparison with global observables	8
<b>5. General features of the distribution</b>	<b>9</b>
5.1 Iterative solution at small $\Delta$	9
5.2 Asymptotic behaviour at large $\Delta$	10
5.3 Numerical results	12
<b>6. Study of the large-<math>\Delta</math> behaviour</b>	<b>12</b>
6.1 Shape of the peak at $a=b$	13
6.2 The distribution off the peak	15
6.3 Small $\mathcal{C}_{\text{in}}$ region	17
<b>7. Discussion</b>	<b>18</b>
<b>A. Interjet observables in DIS and hadron-hadron collisions</b>	<b>21</b>
A.1 The observable	21
A.2 QCD resummation: DIS case	21
A.3 QCD resummation: hadron-hadron case	22
<b>B. Theorem: <math>0 \leq G_{ab}(\Delta) \leq 1</math></b>	<b>24</b>
<b>C. Iterative solution</b>	<b>25</b>

---

## 1. Introduction

Study of “interjet” hadronic emission [1, 2, 3] is of special interest in QCD. In general, such emission originates from the flow of colour between jets, and therefore its analysis is important for understanding the mechanism of the overall colour neutralization. In practical terms, the interjet radiation is typically soft and so the distributions are

sensitive to possible non-perturbative components such as underlying events. For recent and not-so-recent experimental studies in hadronic colliders, see [4, 5].

A characteristic feature of inclusive interjet distributions is that collinear singularities do not play a relevant rôle and that the distributions are essentially determined by large angle soft emissions, which are responsible for the coherence of QCD radiation [6, 7].

An example of an interjet quantity is  $E_{\text{out}}$ , the total energy (or transverse momentum) of hadrons emitted in a region  $\mathcal{C}_{\text{out}}$  away from all hard jets. The  $E_{\text{out}}$  distribution is infrared (and collinear) safe so that all its perturbative (PT) coefficients are finite and computable (in principle, although the resulting series then does not converge). Typically one has  $E_{\text{out}} \ll Q$ , with  $Q$  the hard scale of the process, so that reliable QCD estimates require the resummation<sup>1</sup> of the logarithmically enhanced terms generated by soft emitted or virtual partons. Since for this observable no logarithms are generated from collinear singularities, one has that the leading contributions to the distribution are given by single logarithmic (SL) terms  $\alpha_s^n \ln^n Q/E_{\text{out}}$ .

This should be contrasted with the case of observables in which the measured region includes one or more jets. An example of this is the thrust in the  $e^+e^-$  process. In such cases both soft and collinear singularities contribute, so that the logarithm of the distribution contains, besides SL terms, also double logarithmic (DL) terms ( $\alpha_s^n L^{n+1}$  with  $L$  a large logarithm).

Typically one expects that less singular distributions would be more difficult to resum. This is actually the case here. For a distribution in a “global” observable, i.e. involving the entire phase space, the PT expansion can be resummed [8] by means of a *linear* evolution equation (a generalization of the DGLAP equation [9]) based on the factorization of collinear singularities and coherence of the QCD branching structure [6, 7]. The resulting distribution can be expressed as a Sudakov form factor (the exponential of a *radiator*) which corresponds to bremsstrahlung emission directly from the primary partons.

As shown by Dasgupta and Salam [10], “non-global” observables<sup>2</sup>, i.e. involving a part of the phase space, cannot be described only by the bremsstrahlung process but they involve the entire structure of successive parton branching. Calculations in  $e^+e^-$  and DIS were performed numerically by a Monte Carlo method based on dipole branching emission derived from the distribution of many soft gluons emitted off a colour singlet dipole of hard partons given in [7, 11] in the large  $N_c$  limit.

Given the relevance of interjet observables, it would be important to have an analytic formulation for the SL resummation and this is the aim of the present study.

---

<sup>1</sup>Only the average value of  $E_{\text{out}}$  or the distribution for relatively large  $E_{\text{out}}$  are obtained by finite order calculations [1].

<sup>2</sup>Interjet observables are a particular case of non-global observable. Their numerical study for  $e^+e^-$  has been performed in [2].

We derive an evolution equation based on the soft multi-gluon distribution given in [7, 11] valid for soft emissions in all angular regions. This evolution equation resums all SL contributions for the interjet distribution. It is based on energy ordering but implies also angular ordering [6, 7], which is the basis of Monte Carlo QCD simulations [12]. As in [2] this formulation of the branching involves colour singlet dipoles in the large  $N_c$  approximation.

In the main text we consider the case of  $e^+e^-$  annihilation with an unobserved region  $\mathcal{C}_{\text{in}}$  defined by a cone around the thrust axis. Our analysis is extended in Appendix A to processes with incoming hadrons such as DIS and hadron-hadron collisions with large  $P_t$ -jets. We show that for all these hard processes the interjet distributions are given (in the large  $N_c$  limit) in terms of a single function which depends on the geometry of the process.

We derive the shape of the interjet distribution for large  $Q/E_{\text{out}}$  and the structure of the branching and we discuss emission into the  $\mathcal{C}_{\text{out}}$  region. We characterize these aspects in terms of quantities which are either universal or geometry-dependent. We confirm features found in [2] in numerical studies.

The paper is organized as follows. In section 2 we describe the observable we consider and in section 3 we express the interjet distribution in terms of soft multiparton emission. In section 4 we derive the evolution equation and we compare the case of the interjet distribution with the ones of other observables. In section 5 we describe the general features of the distribution, with both analytical and numerical methods. Section 6 contains the detailed technical discussion for large  $Q/E_{\text{out}}$ . Universal and geometry-dependent features are derived. Finally, in section 7 we recall the main physical features of the interjet distribution.

## 2. The observable

For a given hard process we consider as our interjet observable the total energy of hadrons emitted in a phase space region  $\mathcal{C}_{\text{out}}$  away from all hard jets

$$E_{\text{out}} = \sum_{h \in \mathcal{C}_{\text{out}}} \omega_h . \quad (2.1)$$

Most of the energy flows inside the jet regions so that typically we have  $E_{\text{out}} \ll Q$  with  $Q$  the hard scale. The features we will describe for this observable can be extended to other interjet observables such as the total hadron transverse energy. The interjet region  $\mathcal{C}_{\text{out}}$  could be defined in various ways according to the hard process. The complementary region including the jets will be denoted by  $\mathcal{C}_{\text{in}}$ .

In  $e^+e^-$  annihilation we will consider the interjet region  $\mathcal{C}_{\text{out}}$  as

$$-\cos \theta_{\text{in}} < \cos \theta_h < \cos \theta_{\text{in}} , \quad (2.2)$$

with  $\theta_h$  the angle with respect to the thrust axis  $\vec{n}_T$ . We will discuss the following collinear and infrared safe distribution

$$\Sigma_{e^+e^-}(E_{\text{out}}) = \sum_n \int \frac{d\sigma_n}{\sigma_T} \cdot \Theta \left( E_{\text{out}} - \sum_{h \in \mathcal{C}_{\text{out}}} \omega_h \right), \quad (2.3)$$

with  $d\sigma_n$  the  $n$ -hadron distribution and  $\sigma_T$  the total cross section. The dependence on  $\theta_{\text{in}}$  and  $Q$  is understood. This distribution is normalized to one at the kinematical limit  $E_{\text{out}} \sim Q$ . The process is dominated by two-jet events aligned along the thrust axis so that  $E_{\text{out}}$  is typically much smaller than  $Q$ . Three-jet events, with  $E_{\text{out}} \sim Q$ , are of order of  $\alpha_s(Q)$ .

In Appendix A we discuss examples of a similar interjet observable in DIS and hadron-hadron collisions with high  $P_t$ -jets.

### 3. QCD resummation

At parton level, for small  $E_{\text{out}}$  the distribution in  $e^+e^-$  is described by the emission of the primary quark-antiquark pair  $p\bar{p}$  accompanied by secondary soft gluons  $k_i$ ,

$$e^+e^- \rightarrow p k_1 \dots k_n \bar{p}. \quad (3.1)$$

In the soft limit, the primary quark and antiquark are aligned along the thrust axis. The leading contribution of the soft multi-parton distribution  $M_n^2$  is obtained by considering strong energy ordering for the emitted partons. Here, the phase space integration can be approximated by ( $E \sim Q$ )

$$d\Phi_n = \prod_i \omega_i d\omega_i \frac{d^2\Omega_i}{4\pi} \Theta(E - \omega_i). \quad (3.2)$$

For any one of the  $n!$  strongly energy-ordered regions, the real emission contribution to the soft multi-parton distribution is given, in the large  $N_c$  limit, by the factorized expression (see [7, 11])

$$\begin{aligned} M_n^2(pk_1 \dots k_n \bar{p}) &= M_0^2(p\bar{p}) \cdot S_{p\bar{p}}(k_1 \dots k_n), \\ S_{p\bar{p}}(k_1 \dots k_n) &= \frac{1}{n!} \prod_i \frac{\bar{\alpha}_s}{\omega_i^2} \sum_{\pi_n} W_n(pk_{i_1} \dots k_{i_n} \bar{p}), \quad \bar{\alpha}_s = N_c \frac{\alpha_s}{\pi}, \end{aligned} \quad (3.3)$$

where the sum is over all  $n!$  permutations. For the fundamental permutation we have

$$W_n(pk_1 \dots k_n \bar{p}) = \frac{(p\bar{p})}{(pk_1)(k_1 k_2) \dots (k_n \bar{p})}, \quad (qq') \equiv 1 - \cos \theta_{qq'}. \quad (3.4)$$

This distribution has both soft ( $\omega_i \rightarrow 0$ ) and collinear ( $\theta_{qq'} \rightarrow 0$ ) singularities. It is valid in any strongly energy-ordered region. No collinear approximations are involved in the derivation, so it is valid even at large angles as needed for our study.

To leading order for small  $E_{\text{out}}$ , the distribution  $\Sigma_{e^+e^-}(E_{\text{out}})$  is obtained by using

$$\frac{d\sigma_n}{\sigma_T} = S_{p\bar{p}}(k_1 \dots k_n) \cdot d\Phi_n. \quad (3.5)$$

Here we have to add to the soft distribution given in (3.3) the virtual corrections to the same order in the soft limit. This will be done in the next section in which we derive the evolution equation giving  $\Sigma_{e^+e^-}(E_{\text{out}})$ . The expression (3.5), being accurate at the leading order in the soft limit, contains all the SL terms we want to resum.

The basis for the resummation is the factorized structure of  $M_n^2$ . We then factorize<sup>3</sup> also the theta function in (2.3) by writing

$$\Theta \left( E_{\text{out}} - \sum_{i \in \mathcal{C}_{\text{out}}} \omega_i \right) = \int \frac{d\nu e^{\nu E_{\text{out}}}}{2\pi i \nu} \prod_i u(k_i), \quad u(k) = \Theta_{\text{in}}(k) + e^{-\nu\omega} \Theta_{\text{out}}(k), \quad (3.6)$$

where  $\Theta_{\text{out}}(k)$  and  $\Theta_{\text{in}}(k)$  are the support functions in the interjet region  $\mathcal{C}_{\text{out}}$  and  $\mathcal{C}_{\text{in}}$  respectively. The geometry of the interjet region  $\mathcal{C}_{\text{out}}$ , i.e. the  $\theta_{\text{in}}$  dependence, is totally contained in the source  $u(k)$ . The distribution is then given by

$$\Sigma_{e^+e^-}(E_{\text{out}}) = \int \frac{d\nu e^{\nu E_{\text{out}}}}{2\pi i \nu} G_{p\bar{p}}(E, \nu^{-1}) \simeq G_{p\bar{p}}(E, E_{\text{out}}), \quad (3.7)$$

where the Mellin variable  $\nu$  runs along the imaginary axis to the right of the singularities of  $G_{p\bar{p}}(E, \nu^{-1})$ . In (3.7) we have evaluated the Mellin integration by steepest descent to give  $\nu \simeq E_{\text{out}}^{-1}$ . The contribution from real emission (3.3) is given by

$$G_{p\bar{p}}^{(\text{real})}(E, E_{\text{out}}) = 1 + \sum_{n=1}^{\infty} \int \prod_{i=1}^n \left\{ \bar{\alpha}_s \frac{d\omega_i}{\omega_i} \frac{d^2\Omega_i}{4\pi} u(k_i) \Theta(E - \omega_i) \right\} W_n(pk_1 \dots k_n \bar{p}). \quad (3.8)$$

Here we set  $\nu = E_{\text{out}}^{-1}$  in the source  $u(k)$  and used the symmetry in the secondary gluons to select the fundamental permutation at the cost of the  $1/n!$  factor. Virtual corrections to (3.8) will be introduced in the next section.

In Appendix A we extend this analysis to hard processes with incoming hadrons and show that interjet distributions for all hard processes are described by the same function  $G_{p_i p_j}(E, E_{\text{out}})$  with  $p_i$  and  $p_j$  the direction of pairs of hard jets (incoming or outgoing) and on the interjet region  $\mathcal{C}_{\text{out}}$ .

## 4. Evolution equation

To formulate an evolution equation we need to introduce the distribution  $G_{ab}$  for a general pair of primary partons  $p_a p_b$ , obtained from (3.8) by replacing  $p\bar{p}$  by generic

<sup>3</sup>Alternatively, we can use strong energy ordering so that  $E_{\text{out}}$  is the energy of the hardest secondary soft gluon. The Mellin transform method simplifies the combinatorics.

dipole momenta  $p_a p_b$ . This distribution depends on the direction of  $p_a p_b$  with respect to the  $e^+ e^-$  thrust axis and on the geometry of the interjet region  $\mathcal{C}_{\text{out}}$ , i.e. on  $\theta_{\text{in}}$  in (2.2). To obtain the evolution equation we use

$$E \partial_E \left\{ W(p_a k_1 \dots k_n p_b) \prod_{i=1}^n \Theta(E - \omega_i) \right\} = \sum_{\ell=1}^n E \delta(E - \omega_\ell) w_{ab}(k_\ell) \cdot \left\{ W(p_a k_1 \dots k_\ell) \prod_{i=1}^{\ell-1} \Theta(E - \omega_i) \right\} \cdot \left\{ W(k_\ell \dots k_n p_b) \prod_{i=\ell+1}^n \Theta(E - \omega_i) \right\}, \quad (4.1)$$

where

$$w_{ab}(k) = \frac{(p_a p_b)}{(p_a k)(k p_b)} = \frac{1 - \cos \theta_{ab}}{(1 - \cos \theta_{ak})(1 - \cos \theta_{kb})}. \quad (4.2)$$

We then deduce the basic equation ( $\nu = E_{\text{out}}^{-1}$  dependence is understood)

$$E \partial_E G_{ab}(E) = \int \frac{d^2 \Omega_k}{4\pi} \bar{\alpha}_s w_{ab}(k) [u(k) G_{ak}(E) \cdot G_{kb}(E) - G_{ab}(E)]. \quad (4.3)$$

Here we have added virtual corrections, the last term in the square bracket, to the same order as the real emission contributions, see [7]. This evolution equation corresponds to soft dipole emission with energy ordering. Since  $w_{ab}(k)$  effectively constrains  $k$  into the angular region within the  $ab$  dipole, (4.3) also implies angular ordering (after azimuthal averaging). Large angle regions are correctly taken into account.

It is convenient to write (4.3) in the form

$$E \partial_E G_{ab}(E) = -E \partial_E R_{ab}^{(0)}(E) \cdot G_{ab}(E) + \int \frac{d^2 \Omega_k}{4\pi} \bar{\alpha}_s w_{ab}(k) u(k) [G_{ak}(E) \cdot G_{kb}(E) - G_{ab}(E)], \quad (4.4)$$

with  $R_{ab}^{(0)}(E)$  the SL Sudakov radiator for the bremsstrahlung emission

$$R_{ab}^{(0)}(E) = \int_0^E \frac{d\omega}{\omega} \int \frac{d^2 \Omega_k}{4\pi} \bar{\alpha}_s w_{ab}(k) [1 - u(k)] = \Delta \cdot r_{ab}, \quad (4.5)$$

where  $\Delta$  depends on  $E, E_{\text{out}}$  and  $r_{ab}$  on the geometry of the interjet region (2.2)

$$\Delta = \int_0^E \frac{d\omega}{\omega} \bar{\alpha}_s [1 - e^{-\omega/E_{\text{out}}}], \quad r_{ab} = \int_{\mathcal{C}_{\text{out}}} \frac{d^2 \Omega_k}{4\pi} w_{ab}(k). \quad (4.6)$$

Here we have used  $[1 - u(k)] = [1 - e^{-\omega/E_{\text{out}}}] \Theta_{\text{out}}(k)$  which entails that, in the unobserved jet region  $\mathcal{C}_{\text{in}}$ , the infrared and collinear singularities of  $w_{ab}(k)$  are fully cancelled between real and virtual contributions.

In the quantity  $\Delta$  the argument of the running coupling  $\alpha_s$  is determined by the successive hard emission contributions and cannot be determined in the present analysis. Detailed analysis [13] shows that, in the physical scheme, it is given by the transverse momentum relative to the  $ab$ -dipole which here can be approximated by the energy since the contributions to this radiator come from large angle emission.

For small  $E_{\text{out}}$  we can evaluate  $\Delta$  by the standard SL approximation

$$1 - e^{-\nu\omega} \simeq \Theta(\omega - e^{\gamma_E} \nu^{-1}) \simeq \Theta(\omega - E_{\text{out}}), \quad \Delta \simeq \int_{E_{\text{out}}}^E \frac{d\omega}{\omega} \bar{\alpha}_s. \quad (4.7)$$

The radiator  $R_{ab}^{(0)}$  is then the contribution from the virtual parton in the  $\mathcal{C}_{\text{out}}$  phase space with energy  $\omega \gtrsim E_{\text{out}}$ . For fixed  $\alpha_s$  we have  $\Delta \simeq \bar{\alpha}_s \ln E/E_{\text{out}}$ .

The evolution equation (4.4) does not generate any collinear logarithms, either from the bremsstrahlung factor  $r_{ab}$  (since the region  $\mathcal{C}_{\text{out}}$  does not include  $p_a$  or  $p_b$ ) or from the integral term in the second line of (4.4). The latter is collinear regular due to cancellation between the branching  $G_{ak} \cdot G_{kb}$  and the virtual  $-G_{ab}$  terms. Indeed, for  $k$  collinear to  $p_a$  one has  $G_{ak} \rightarrow 1$  and  $G_{kb} \rightarrow G_{ab}$  so that the sum in the square brackets vanishes and regularizes the singularity of  $w_{ab}(k)$ . Since only soft singularities remain, the leading terms of  $G_{ab}$  are SL contributions.

To SL order, we can replace  $u(k)$  by  $\Theta_{\text{in}}(k)$  in the integral term of (4.4). To show this observe that the remaining piece  $e^{-\omega/E_{\text{out}}} \Theta_{\text{out}}(k)$  of the source contributes with energy  $\omega \lesssim E_{\text{out}}$  (see (4.7)) while the softest gluon, which contributes to  $R_{ab}^{(0)}$ , has a typically larger energy ( $\omega \gtrsim E_{\text{out}}$ ). We conclude that the soft secondary branching takes place in  $\mathcal{C}_{\text{in}}$  and only the final parton enters the interjet region  $\mathcal{C}_{\text{out}}$  and here it contributes only with the virtual correction with energy  $\omega \gtrsim E_{\text{out}}$ .

By replacing  $u(k) \rightarrow \Theta_{\text{in}}(k)$  in the branching term of (4.4) we have that the distribution  $G_{ab}$  depends on  $E$  and  $E_{\text{out}}$  only through the function  $\Delta$ . We then can replace  $G_{ab}(E, E_{\text{out}}) \rightarrow G_{ab}(\Delta)$  and obtain, to SL accuracy,

$$\partial_\Delta G_{ab}(\Delta) = -r_{ab} G_{ab}(\Delta) + \int_{\mathcal{C}_{\text{in}}} \frac{d^2\Omega_k}{4\pi} w_{ab}(k) [G_{ak}(\Delta) \cdot G_{kb}(\Delta) - G_{ab}(\Delta)], \quad (4.8)$$

with the initial condition  $G_{ab}(\Delta=0)=1$ . The distribution  $G_{ab}(\Delta)$  can be factorized into two pieces

$$G_{ab}(\Delta) = e^{-R_{ab}^{(0)}(\Delta)} \cdot g_{ab}(\Delta). \quad (4.9)$$

The first is the Sudakov factor given by bremsstrahlung emission from the primary hard partons  $p_a p_b$ . The second factor is the result of successive soft secondary branching which satisfies

$$\partial_\Delta g_{ab}(\Delta) = \int_{\mathcal{C}_{\text{in}}} \frac{d^2\Omega_k}{4\pi} w_{ab}(k) \left[ U_{abk}^{(0)}(\Delta) g_{ak}(\Delta) \cdot g_{kb}(\Delta) - g_{ab}(\Delta) \right], \quad (4.10)$$



where

$$U_{abk}^{(0)}(\Delta) = e^{-R_{ak}^{(0)}(\Delta) - R_{kb}^{(0)}(\Delta) + R_{ab}^{(0)}(\Delta)}, \quad (4.11)$$

is an effective source. Notice that (4.10) has the same structure as (4.3) with  $u$  replaced by  $U^{(0)}$ . The factorization in (4.9) can then be iterated, see later.

#### 4.1 Comparison with global observables

The evolution equation (4.4) can be generalized to any collinear and infrared safe observable. Consider for example an additive global observable

$$V = \sum_i v(k_i), \quad (4.12)$$

with  $v(k_i)$  a function of the emitted hadron momentum. One deduces<sup>4</sup> again (4.4) with the bremsstrahlung radiator involving the source for the specific observable

$$R_{ab}^{(0)}(E) = \int_0^E \frac{d\omega}{\omega} \int \frac{d^2\Omega_k}{4\pi} \bar{\alpha}_s w_{ab}(k) [1 - e^{-\nu v(k)}]. \quad (4.13)$$

This quantity is collinear and infrared safe if  $v(k_i)$  vanishes for  $k_{ti} \rightarrow 0$ . In this case the radiator involves also double logarithmic contributions  $\alpha_s^n \ln^{n+1} V$  which arise from the collinear and infrared singular structure of  $w_{ab}(k)$ . SL terms coming from hard collinear emission are not included in (4.13), but these can easily be included by adding to  $w_{ab}(k)$  the finite pieces of the splitting functions.

The soft secondary branching in the evolution equation (second line in (4.4)) plays a very different rôle<sup>5</sup> for global and local observables. As previously discussed, for local observables all soft secondary branching terms contribute to SL accuracy. For global observables, instead, soft secondary branching contributes beyond SL accuracy [6, 7]. This fact can be easily seen in the present formulation.

Consider for instance the two loop contribution which involves the combination of the sources  $u(k_2)[1 - u(k_1)]$  with  $\omega_1 < \omega_2$ . For the local observable  $E_{\text{out}}$  here considered, we have that  $u(k_2)[1 - u(k_1)]$  is consistent with energy ordering provided  $k_1 \in \mathcal{C}_{\text{out}}$  and  $k_2 \in \mathcal{C}_{\text{in}}$  so that one has a SL contribution  $\alpha_s^2 \ln^2 E/E_{\text{out}}$ . For a global observable instead, with  $\mathcal{C}_{\text{in}} = 0$ , we have that the combination  $u(k_2)[1 - u(k_1)]$  contributes in the region  $v(k_2) > v(k_1)$  (see (4.7)) which is in conflict with energy ordering. As a result, secondary branching has no infrared logarithms and one remains with a subleading term,  $\alpha_s^2 \ln V$ , which comes from the collinear singularity of the dipole emission. As a result for a global observable, the distribution is simply given by a Sudakov form factor, the exponentiation of the DL bremsstrahlung radiator.

<sup>4</sup>In general one may need to factorize phase space constraints also, see [8].

<sup>5</sup>As recalled before, the present treatment does not include hard contributions from the secondary branching which reconstruct the running coupling argument.

In (2.3) we have considered interjet observables in which  $\mathcal{C}_{\text{out}}$  does not include the primary parton region. The analysis can be generalized to the case in which the phase space region defining the local observable includes one primary parton [10]. Here one has DL contributions and soft secondary branching giving SL terms to all orders.

## 5. General features of the distribution

We cannot solve analytically the SL evolution equation (4.8). However we can study various aspects of the distribution using different approaches to give a picture of how the distribution behaves. We first observe that the distribution satisfies the constraint

$$0 \leq G_{ab}(\Delta) \leq 1, \quad (5.1)$$

for any  $\Delta$  and  $ab$ . A proof of this is given in Appendix B. We also know that  $G_{ab}(0) = 1$  and that, since the  $ab$ -dipole does not emit for  $a=b$  we have

$$G_{ab}(\Delta) \rightarrow 1, \quad \text{for } a \rightarrow b, \quad (5.2)$$

for any  $\Delta$ . For  $a \neq b$ ,  $G_{ab}(\Delta) \rightarrow 0$  as  $\Delta$  becomes large. This implies that the distribution  $G_{ab}(\Delta)$  has a peak at  $a=b$ , whose width decreases with increasing  $\Delta$ . This peak governs the evolution of the entire distribution.

We have used three approaches to study the distribution: an iterative solution valid at small  $\Delta$ , the asymptotic behaviour at large  $\Delta$ , and numerical solution. We discuss the results in the following subsections.

### 5.1 Iterative solution at small $\Delta$

We observe that (4.10) for  $g_{ab}$  is similar to (4.3) for  $G_{ab}$  with  $u(k)$  replaced by  $U_{abk}^{(0)}$  defined in (4.11). By iterating the procedure used to factorize the bremsstrahlung piece (see (4.9)) we obtain the general expansion

$$g_{ab}(E) = \exp \left( - \sum_{n=1}^{\infty} R_{ab}^{(n)}(\Delta) \right), \quad (5.3)$$

with the radiator components defined iteratively by

$$R_{ab}^{(n+1)}(\Delta) = \int_0^\Delta d\Delta' \int_{\mathcal{C}_{\text{in}}} \frac{d^2\Omega_k}{4\pi} w_{ab}(k) \prod_{i=0}^{n-1} U_{abk}^{(i)}(\Delta') \left[ 1 - U_{abk}^{(n)}(\Delta') \right], \quad (5.4)$$

$$U_{abk}^{(i)}(\Delta) = e^{-R_{ak}^{(i)}(\Delta) - R_{kb}^{(i)}(\Delta) + R_{ab}^{(i)}(\Delta)}.$$

We see immediately that at small  $\Delta$ ,  $R_{ab}^{(n)}(\Delta)$  is of order  $\Delta^{n+1}$  so that all terms contribute to SL accuracy. This is the crucial difference with the case for global

observables in which the soft secondary branching contributes beyond SL level, see discussion in subsection 4.1.

In Appendix C we compute the first term for the  $e^+e^-$  physical distribution  $R_{p\bar{p}}^{(1)}(\Delta)$ . At small  $\Delta$  we find (see [2])

$$R_{p\bar{p}}^{(1)}(\Delta) = \Delta^2 \left( \frac{\pi^2}{12} - \frac{\text{Li}_2(\tan^4 \frac{\theta_{\text{in}}}{2})}{2} \right) + \mathcal{O}(\Delta^3) , \quad (5.5)$$

while at large  $\Delta$  it becomes

$$R_{p\bar{p}}^{(1)}(\Delta) = \Delta \ln \left( \Delta e^{\gamma_E - 1} (1 - \tan^4 \frac{\theta_{\text{in}}}{2}) \right) + \mathcal{O}(1) . \quad (5.6)$$

As  $\Delta$  increases, the higher contributions will also become important. However it is interesting to note the dependence on  $\theta_{\text{in}}$  – even for quite large  $\theta_{\text{in}}$  (of order 1) the distribution  $R_{p\bar{p}}^{(1)}$  is relatively insensitive to it, and in order to get a noticeable  $\theta_{\text{in}}$ -dependence one has to move close to the limit  $\theta_{\text{in}} = \frac{\pi}{2}$ .

## 5.2 Asymptotic behaviour at large $\Delta$

The most physically interesting study is of the behaviour at large  $\Delta$ , which is discussed at length in section 6. Here we summarise the method and important results.

To a first and quite crude approximation, we may treat  $G_{ab}(\Delta)$  at large  $\Delta$  as being approximately 1 around  $a=b$ , and very small elsewhere, in other words having a peak of height 1 at  $a=b$ . This cuts off the integral in equation (4.8) for the secondary emission  $k$  near the emitters  $a$  or  $b$ . Physically this means that real gluons are only emitted close to one of the emitters; in the other regions only virtual gluons contribute. This is the same effect as described in [2], where from numerical results it was seen that secondary gluons were radiated in a region around the primary partons, but that there also existed a large empty “buffer” region extending to the edge of  $\mathcal{C}_{\text{in}}$ . Importantly, this also means that the geometry of the  $\mathcal{C}_{\text{in}}$  region becomes less important, since what determines if a gluon is emitted or not in a particular direction is no longer whether that direction is in  $\mathcal{C}_{\text{in}}$  or  $\mathcal{C}_{\text{out}}$ , but if it is within the peak around one of the primary emitters or not. Thus we find that the leading large- $\Delta$  behaviour is independent of geometry. (Of course subleading terms are still geometry-dependent.)

Of particular physical importance is the width of the distribution peak, which is a measure of the size of the buffer. We quantify this in terms of a critical angle  $\theta_{\text{crit}}(\Delta)$  around parton  $a$ . Then we introduce a function  $h_\Delta(z)$  which for large  $\Delta$  we take to give the shape of the peak with normalised width. We derive coupled evolution equations for  $\theta_{\text{crit}}(\Delta)$  and  $h_\Delta(z)$  which we evolve numerically to give what we assume to be stable limits for  $d \ln \theta_{\text{crit}}/d\Delta$  and  $h_\infty(z)$ . At large  $\Delta$  we then find

$$\theta_{\text{crit}}(\Delta) \simeq \lambda_a(\mathcal{C}_{\text{in}}) \cdot e^{-\frac{\epsilon}{2}\Delta} , \quad (5.7)$$

where  $c \approx 2.5$  is a universal constant. The subleading behaviour, and in particular the normalization constant  $\lambda_a$ , is dependent on the geometry of  $\mathcal{C}_{\text{in}}$  and on the position of parton  $a$ , see section 6. Thus at large  $\Delta$  the region within  $\theta_{\text{crit}}(\Delta)$  rapidly shrinks and the interjet region  $\mathcal{C}_{\text{in}}$  becomes more and more empty. This compares well with [2], who suggest from the numerical analysis the same functional form, with a value for  $c$  of about 3 (which is probably consistent within errors).

Then using the asymptotic peak shape  $h_\infty(z)$  we obtain the large- $\Delta$  behaviour for the whole distribution. Consider the physical distribution for a general hard process given in terms of  $G_{p_i p_j}(\Delta)$  with  $p_i$  and  $p_j$  the hard primary jet directions which in general form an angle  $\theta_{ij}$ . We derive the following Gaussian behaviour at large  $\Delta$

$$G_{p_i p_j}(\Delta) \simeq e^{-\frac{c}{2}\Delta^2} \left( \frac{\lambda_i \lambda_j e^{-c'}}{1 - \cos \theta_{ij}} \right)^\Delta \cdot f_{ij}, \quad (5.8)$$

Here  $c$  is the same universal constant in (5.7) and  $c'$  a second universal constant. The functions  $f_{ij}$  and  $\lambda_i, \lambda_j$  depend on the geometry  $\mathcal{C}_{\text{in}}$  and the jet directions. They arise as integration constants in the large  $\Delta$  approximation of the evolution equation.

When the excluded jet region  $\mathcal{C}_{\text{in}}$  is a pair of small cones of angle  $\theta_{\text{in}}$  centred on the jet directions  $p_i p_j$  the width of the peak becomes proportional to  $\theta_{\text{in}}$

$$\lambda_i(\mathcal{C}_{\text{in}}) = \lambda_j(\mathcal{C}_{\text{in}}) = \theta_{\text{in}} \cdot \hat{\lambda}_0. \quad (5.9)$$

We obtain

$$G_{p_i p_j}(\Delta) \simeq \left( \frac{\theta_{\text{in}}^2}{2(1 - \cos \theta_{ij})} \right)^\Delta \cdot g(\Delta), \quad g(\Delta) \simeq e^{-\frac{c}{2}\Delta^2} \left( 2\hat{\lambda}_0^2 e^{-c'} \right)^\Delta \hat{f}_0^2. \quad (5.10)$$

At large  $\Delta$  the Gaussian behaviour coming from the soft secondary emission dominates over the bremsstrahlung contribution, which is the first factor. For small  $\theta_{\text{in}}$  the soft secondary branching distribution  $g(\Delta)$  becomes fully  $\theta_{\text{in}}$ -independent and direction-independent. The constants  $\hat{f}_0, \hat{\lambda}_0$  arise one factor from each jet, since for small  $\mathcal{C}_{\text{in}}$  the two jet contributions factorize, and by symmetry they are equal. Thus in any hard QCD process the distribution of energy emitted into the region excluding a narrow cone around each hard jet is determined for each colour flow by the usual bremsstrahlung radiator multiplied once for each emitting dipole by the universal Gaussian function  $g(\Delta)$ .

If the weak dependence of  $R_{pp}^{(1)}(\Delta)$  on  $\theta_{\text{in}}$  found in (5.6) is at all indicative of the general behaviour, we may hope that the small cone approximation (5.10) for  $g(\Delta)$  could be valid even for quite large cones: this was indeed seen in [2]. This smooth behaviour is explained by the fact that for small  $\theta_{\text{in}}$  the critical region  $\theta_{\text{crit}}(\Delta)$  inside which the branching develops scales proportionally to  $\theta_{\text{in}}$ , see (5.9).

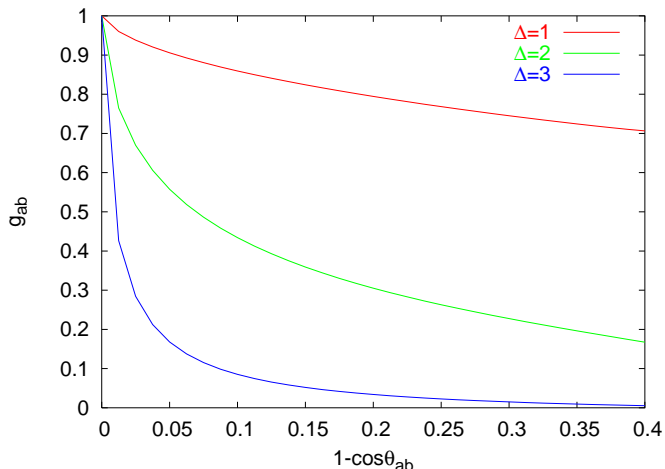


**Figure 1:** The distribution  $g_{ab}$  for  $\cos \theta_{\text{in}} = \frac{1}{2}$  and  $\theta_a = 0$  as a function of  $1 - \cos \theta_{ab}$  for three different values of  $\Delta$ .

### 5.3 Numerical results

We try a numerical solution of (4.10) to give the quantitative behaviour of the secondary branching distribution  $g_{ab}(\Delta)$  in  $e^+e^-$  annihilation. We set a grid of 40 bins in  $\phi$  and 80 bins in  $\cos \theta$  and evolve (4.10) numerically. Real-virtual cancellation is implemented by neglecting the contribution with  $k = a$  or  $k = b$  in (4.10). This may be a crude approximation, due to the sharp behaviour of the function  $g_{ab}$  for  $a$  near  $b$ , and needs improvement in order to have complete control on the errors. For what concerns the  $\Delta$  behaviour of the solution, we find substantial agreement with the results obtained in [2].

As stated in the previous subsection, it is crucial to understand the behaviour of the function  $g_{ab}$  when we vary the opening angle between  $a$  and  $b$ . In figure 1 we plot  $g_{ab}$  as a function of  $1 - \cos \theta_{ab}$  for three different values of  $\Delta$ . We choose to fix  $a$  along the thrust axis and let  $\theta_{ab}$  run from 0 to  $\theta_{\text{in}}$ . This distribution starts from 1 and then steeply decreases with increasing  $\theta_{ab}$ . This behaviour confirms the presence of a peak for the  $g_{ab}$  distribution near  $a = b$  which shrinks with increasing  $\Delta$ . The form of this distribution for large  $\Delta$  will be discussed in detail in the next section. From this figure we see that the asymptotic behaviour is already settled at  $\Delta = 3$  where the distribution is negligible away from the peak.

## 6. Study of the large- $\Delta$ behaviour

We focus on  $e^+e^-$  annihilation with  $\mathcal{C}_{\text{in}}$  given by a cone of size  $\theta_{\text{in}}$  around the two jets along thrust axis, see (2.2). We then generalize this analysis to the distribution  $G_{p_i p_j}$  required for other hard processes, in which the two jets are not back-to-back. To obtain  $G_{ab}(\Delta)$  in the large  $\Delta$  limit we need first to study its behaviour near the

peak at  $a=b$ . Using this information we can obtain the asymptotic behaviour of  $G_{ab}$  for any  $a, b$ . These two stages are described in the next two subsections. In a final subsection we consider the particular case of  $\mathcal{C}_{\text{in}}$  being a pair of small cones.

### 6.1 Shape of the peak at $a=b$

For each point  $a$  inside the jet region  $\mathcal{C}_{\text{in}}$ , we can measure the width of the peak in  $b$  near  $a$  by using

$$\int_{\mathcal{C}_{\text{in}}} \frac{d^2\Omega_b}{4\pi} G_{ab}(\Delta) \equiv 1 - \cos \theta_{\text{crit}}(\Delta) \approx \frac{1}{2}\theta_{\text{crit}}^2(\Delta). \quad (6.1)$$

In general this quantity depends on the geometry of the  $\mathcal{C}_{\text{in}}$  region and on the point  $a$  chosen in  $\mathcal{C}_{\text{in}}$ . Here  $\theta_{\text{crit}}(\Delta)$  measures the angle between  $a$  and  $b$  above which the distribution  $G_{ab}$  is suppressed. It is therefore a small angle which decreases as  $\Delta$  increases. We have the initial value  $\theta_{\text{crit}}(\Delta=0)=\theta_{\text{in}}$ .

Since the evolution of the peak is determined only by the distribution around the peak, and not by points remote in phase-space, we have that the shape of the peak in  $G_{ab}(\Delta)$  depends only on the angle  $\theta_{ab}$  between  $a$  and  $b$ . To measure this shape, suppose that at large  $\Delta$  and in the region near  $a=b$  the distribution behaves as

$$G_{ab}(\Delta) = h_{\Delta}(z), \quad z = \frac{\theta_{ab}^2}{2\theta_{\text{crit}}^2(\Delta)}, \quad (6.2)$$

for some function  $h_{\Delta}(z)$  that from (6.1) for all large  $\Delta$  must satisfy

$$\int_0^{\infty} dz h_{\Delta}(z) = 1. \quad (6.3)$$

The evolution equation (4.8) simplifies in that the source term involving  $r_{ab}$  is negligible and the integration over solid angle becomes an integration over a flat plane:

$$\begin{aligned} \partial_{\Delta} h_{\Delta}(z) - \frac{d \ln \theta_{\text{crit}}^2}{d\Delta} \cdot z h'_{\Delta}(z) &= \frac{1}{2\pi} \int \frac{dx dy}{r_1^2 r_2^2} [h_{\Delta}(r_1^2 z) h_{\Delta}(r_2^2 z) - h_{\Delta}(z)], \\ r_1^2 = x^2 + y^2, \quad r_2^2 = (1-x)^2 + y^2, \quad \theta_{ak} &= r_1 \theta_{ab}, \quad \theta_{kb} = r_2 \theta_{ab}. \end{aligned} \quad (6.4)$$

Integrating this equation over  $z$  yields

$$\frac{d \ln \theta_{\text{crit}}^2}{d\Delta} = \frac{1}{2\pi} \int_0^{\infty} dz \int \frac{dx dy}{r_1^2 r_2^2} [h_{\Delta}(r_1^2 z) h_{\Delta}(r_2^2 z) - h_{\Delta}(z)]. \quad (6.5)$$

Equations (6.3)-(6.5) form a coupled system that can be evolved numerically from any suitable starting function  $h_0(z)$ . Here  $h_{\Delta}(z)$  is a function of only one variable  $z$  while the full distribution  $G_{ab}(\Delta)$  is a function of three angles, so the implementation is somewhat easier.

There are many possible choices of starting function  $h_0(z)$ : it need only be bounded between 0 and 1, with  $h_0(0) = 1$ , normalised, and sufficiently smooth. We used a selection of such functions, namely

$$h_0(z) = e^{-[z\Gamma(1+\frac{1}{n})]^n}, \quad (n = \frac{1}{2}, 1, 2, 3, 4), \quad h_0(z) = \frac{2-z}{2}\Theta(2-z), \quad (6.6)$$

all of which showed the same asymptotic behaviour. The evolution (6.4) settles down to a shape  $h_\infty(z)$  shown in figure 2, which satisfies the equation

$$c \cdot z h'_\infty(z) = \frac{1}{2\pi} \int \frac{dx dy}{r_1^2 r_2^2} [h_\infty(r_1^2 z) h_\infty(r_2^2 z) - h_\infty(z)] , \quad (6.7)$$

$$c \equiv -\frac{d \ln \theta_{\text{crit}}^2}{d\Delta} = -\frac{1}{2\pi} \int_0^\infty dz \int \frac{dx dy}{r_1^2 r_2^2} [h_\infty(r_1^2 z) h_\infty(r_2^2 z) - h_\infty(z)] \approx 2.5 ,$$

with  $c$  evaluated with an accuracy of about 10%. This error is due to limitations in the numerical analysis from the finite number of  $z$ -points, and the numerical integrals performed at each stage, such that evolving using the same starting function but with a different number of points or precision in the integrals converges to a slightly different numerical value for  $c$ . The step size in  $\Delta$  needs to be small enough to prevent instabilities developing before convergence is seen — we found the value 0.02 to be sufficiently small. The stated uncertainty on the value of  $c$  is a generous estimate. This error could be improved with a more refined analysis.

We then conclude that  $\theta_{\text{crit}}(\Delta)$  has the behaviour at large  $\Delta$  given in (5.7) with  $\lambda_a$  an integration constant which depends on  $\theta_{\text{in}}$  and on the chosen point  $a$ . The fact that  $h_\infty(z)$  is finite for any  $z$  implies that at large  $\Delta$  the distribution  $G_{ab}(\Delta)$  for  $\theta_{ab} \ll 1$  depends on  $\Delta, \theta_{\text{in}}$  and the point  $a$  only through the function  $\theta_{\text{crit}}(\Delta)$ . The function  $h_\infty(z)$  as well as the constant  $c$  is universal.

From the tail of the function  $h_\infty(z)$  at large  $z$  we can estimate the large- $\Delta$  behaviour of  $G_{ab}(\Delta)$  away from the peak in the region

$$\theta_{\text{crit}}(\Delta) \ll \theta_{ab} \ll 1 . \quad (6.8)$$

To obtain this we rewrite equation (6.7) in the form

$$c \cdot \frac{d \ln h_\infty}{d \ln z} = \frac{1}{\pi} \int_{r_1 < r_2} \frac{dx dy}{r_1^2 r_2^2} \left[ h_\infty(r_1^2 z) - 1 + h_\infty(r_1^2 z) \left( \frac{h_\infty(r_2^2 z)}{h_\infty(z)} - 1 \right) \right] . \quad (6.9)$$

As  $z \rightarrow \infty$  the final term in the brackets vanishes and we obtain

$$c \cdot \frac{d \ln h_\infty}{d \ln z} = \int_0^\infty \frac{dz'}{z'} [h_\infty(z') - 1] \xi \left( \frac{z'}{z} \right) , \quad (6.10)$$

with

$$\xi(x) = \begin{cases} \frac{1}{1-x} , & x < \frac{1}{4} , \\ \frac{2}{\pi(1-x)} \tan^{-1} \left( \frac{1-\sqrt{x}}{1+\sqrt{x}} \sqrt{\frac{2\sqrt{x}+1}{2\sqrt{x}-1}} \right) , & x > \frac{1}{4} . \end{cases} \quad (6.11)$$

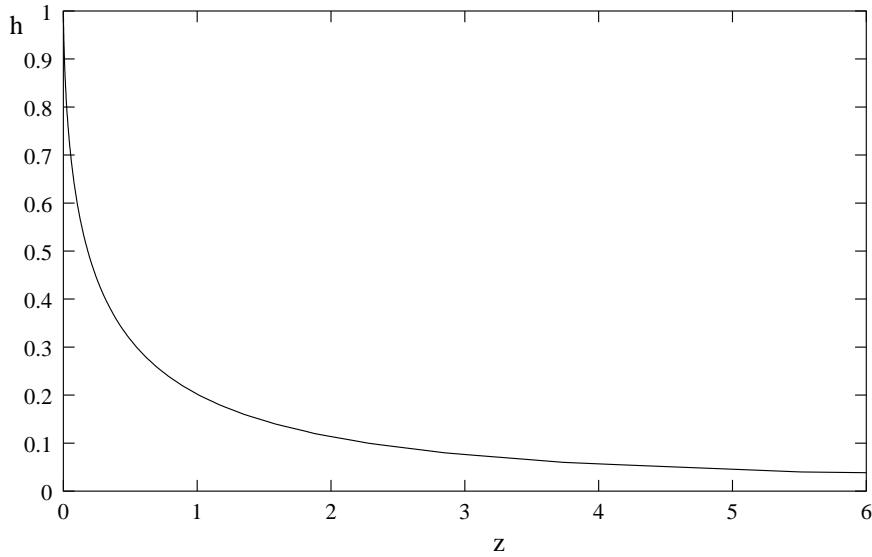


**Figure 2:** The large  $\Delta$  peak,  $h_\infty(z)$ .

In the large  $z$  limit the evolution equation becomes

$$c \cdot \frac{d \ln h_\infty}{d \ln z} \simeq -\ln z - c', \quad c' = \int_0^1 \frac{dz'}{z'} [1 - h_\infty(z')] - \int_1^\infty \frac{dz'}{z'} h_\infty(z'). \quad (6.12)$$

Therefore, using (5.7) and (6.2), we conclude that for  $a$  and  $b$  in the region (6.8) we have, in the large  $\Delta$  limit,

$$\ln G_{ab}(\Delta) \simeq -\frac{c}{2} \Delta^2 - \left( c' + \ln \frac{\theta_{ab}^2}{2\lambda_a^2} \right) \Delta - \left( \frac{c''}{c} + \frac{c'}{c} \ln \frac{\theta_{ab}^2}{2\lambda_a^2} + \frac{1}{2c} \ln^2 \frac{\theta_{ab}^2}{2\lambda_a^2} \right). \quad (6.13)$$

The constants  $c'$  and  $c''$  can be determined by the function  $h_\infty(z)$  shown in figure 2. This behaviour is valid provided  $a, b$  are away from the boundary of  $\mathcal{C}_{\text{in}}$ .

In taking the large- $z$  limit, we have neglected terms that contribute at finite  $z$  in moving from (6.9) to (6.10) and from (6.10) to (6.12). The leading correction is  $\mathcal{O}(z^{-1})$ , and arises from the expansion of the  $\xi$  function in (6.10). Thus the right hand side of (6.13) has a correction  $\mathcal{O}(e^{-c\Delta})$ .

## 6.2 The distribution off the peak

Using the fact that we know the form of  $G_{ab}(\Delta)$  near the peak at  $a = b$ , we now determine the large- $\Delta$  behaviour of  $G_{ab}(\Delta)$  for *any*  $a$  and  $b$  including the physical case in which  $a$  and  $b$  are along the two hard jet directions ( $\theta_{ab} \sim 1$ ).

We find that the geometry dependence in the integration regions of the two terms in (4.8) cancels for large  $\Delta$ . To obtain this result we write (4.8) in the form

$$\partial_\Delta \ln G_{ab} = - \int_{\mathcal{C}_{\text{out}}} \frac{d^2 \Omega_k}{4\pi} w_{ab}(k) + \int_{\mathcal{C}_{\text{in}}} \frac{d^2 \Omega_k}{4\pi} w_{ab}(k) \left( \frac{G_{ak} \cdot G_{kb}}{G_{ab}} - 1 \right). \quad (6.14)$$



Since the first term in the second integral is negligible for  $k$  not near  $a$  or  $b$  we may write

$$\begin{aligned} \partial_\Delta \ln G_{ab} \simeq & - \int_{\theta_{ak}^2, \theta_{kb}^2 > \epsilon} \frac{d^2 \Omega_k}{4\pi} w_{ab}(k) + \int_{\theta_{ak}^2 < \epsilon} \frac{d^2 \Omega_k}{4\pi} w_{ab}(k) \left( \frac{G_{ak} \cdot G_{kb}}{G_{ab}} - 1 \right) \\ & + \int_{\theta_{bk}^2 < \epsilon} \frac{d^2 \Omega_k}{4\pi} w_{ab}(k) \left( \frac{G_{ak} \cdot G_{kb}}{G_{ab}} - 1 \right), \end{aligned} \quad (6.15)$$

where  $\epsilon$  is a small parameter (larger than  $\theta_{\text{crit}}$ ) on which the final answer should not depend. Here we have neglected the ratio  $G_{ak}G_{kb}/G_{ab}$  for  $\theta_{ak}, \theta_{bk} \gg \theta_{\text{crit}}$  which vanishes at large  $\Delta$ . Due to the cancellation of  $\mathcal{C}_{\text{in}}$  and  $\mathcal{C}_{\text{out}}$  in the integration region, we have that, at large  $\Delta$ , the distribution  $G_{ab}(\Delta)$  depends on the geometry and on the directions of  $a$  and  $b$  only through  $\theta_{\text{crit},a}(\Delta)$  and  $\theta_{\text{crit},b}(\Delta)$ , the critical values in (5.7).

We now show that the  $\epsilon$ -dependence in the various terms cancel. The first term of (6.15) gives the contribution with a cutoff around  $a$  and  $b$ : it is, for small  $\epsilon$ ,

$$\int_{\theta_{ak}^2, \theta_{kb}^2 > \epsilon} \frac{d^2 \Omega_k}{4\pi} w_{ab}(k) \simeq \ln \frac{2(1 - \cos \theta_{ab})}{\epsilon}, \quad (6.16)$$

while the second and third terms give the contributions from  $k$  near  $a$  or  $b$ , which depend on the shape of the peak given above. We write

$$\int_{\theta_{ak}^2 < \epsilon} \frac{d^2 \Omega_k}{4\pi} w_{ab}(k) \left( \frac{G_{ak}G_{kb}}{G_{ab}} - 1 \right) \simeq \frac{1}{2} \int_0^\epsilon \frac{d\theta_{ak}^2}{\theta_{ak}^2} (G_{ak} - 1) \simeq -\frac{c'}{2} - \frac{1}{2} \ln \frac{\epsilon}{2\theta_{\text{crit},a}^2}, \quad (6.17)$$

with  $\theta_{\text{crit},a}$  the critical angle for the peak around  $a$  and  $c'$  the constant given in (6.12). Here corrections vanish in the large  $\Delta$  limit. A similar equation holds for the integral around  $b$ . Thus the  $\epsilon$  dependence cancels and we obtain the evolution equation at large  $\Delta$ :

$$\partial_\Delta \ln G_{ab} \simeq -c\Delta - c' - \ln \frac{1 - \cos \theta_{ab}}{\lambda_a \lambda_b}. \quad (6.18)$$

The asymptotic behaviour of  $G_{ab}$  is therefore

$$G_{ab}(\Delta) \simeq e^{-\frac{c}{2}\Delta^2} \left( \frac{\lambda_a \lambda_b e^{-c'}}{1 - \cos \theta_{ab}} \right)^\Delta f_{ab}(\theta_{\text{in}}), \quad (6.19)$$

where  $f_{ab}$  is independent of  $\Delta$  at large  $\Delta$ . For  $\theta_{ab} \ll 1$  we have, see (6.13),

$$\ln f_{ab} \simeq - \left( \frac{c''}{c} + \frac{c'}{c} \ln \frac{\theta_{ab}^2}{2\lambda_a^2} + \frac{1}{2c} \ln^2 \frac{\theta_{ab}^2}{2\lambda_a^2} \right). \quad (6.20)$$

Because of this structure, we have that secondary branching is almost collinear to the partons  $a, b$  initiating the branching: in fact no farther away than the width of the peak. This implies that as long as  $a, b$  are not close to the boundary of  $\mathcal{C}_{\text{in}}$  the geometry dependence enters only through the parameter  $\lambda_a$  in  $\theta_{\text{crit}}$ .

### 6.3 Small $\mathcal{C}_{\text{in}}$ region

Since the secondary branching is almost collinear to the hard primary partons it becomes interesting to study the limit  $\theta_{\text{in}} \rightarrow 0$ . In particular we would like to see how the buffer region behaves when the jet region is squeezed. We consider the two cases of  $ab$  in the same and in opposite jet regions.

**Same jet region.** We derive the evolution equation

$$\begin{aligned} \partial_{\Delta} G_{ab} &= -r_{ab} \cdot G_{ab} + \int_{|\vec{k}| < 1} \frac{d^2 \vec{k}}{2\pi} \frac{(\vec{a} - \vec{b})^2}{(\vec{a} - \vec{k})^2 (\vec{k} - \vec{b})^2} [G_{ak} G_{kb} - G_{ab}] , \\ r_{ab} &= \frac{1}{2} \ln \left( 1 + \frac{(\vec{a} - \vec{b})^2}{(1 - a^2)(1 - b^2)} \right) , \quad \vec{a} = \frac{\theta_a}{\theta_{\text{in}}} \vec{n}_a , \quad \vec{b} = \frac{\theta_b}{\theta_{\text{in}}} \vec{n}_b , \end{aligned} \quad (6.21)$$

using rescaled angular variables  $\vec{a}, \vec{b}$ . The contribution to the evolution of  $G_{ab}$  from the branching in the opposite region vanishes for  $\theta_{\text{in}} \rightarrow 0$ . This is an aspect of coherence of the QCD radiation. We notice that the explicit  $\theta_{\text{in}}$  dependence has disappeared from the equation. This implies that  $\theta_{\text{crit}}(\Delta)$  scales with  $\theta_{\text{in}}$  so that

$$\lambda_a(\mathcal{C}_{\text{in}}) = \theta_{\text{in}} \cdot \hat{\lambda}(\vec{a}) , \quad (6.22)$$

giving (5.9) in the case  $\vec{a} = 0$ . We have then that the buffer region still expands by increasing  $\Delta$ . By performing the same analysis as in subsection 6.1 we find, at large  $\Delta$ , for  $ab$  in the same jet region but away from the peak, the behaviour

$$G_{ab}(\Delta) \simeq e^{-\frac{\epsilon}{2}\Delta^2} \left( \frac{2\hat{\lambda}(\vec{a}) \hat{\lambda}(\vec{b}) e^{-c'}}{(\vec{a} - \vec{b})^2} \right)^{\Delta} \hat{f}(\vec{a}, \vec{b}) . \quad (6.23)$$

**Opposite jet regions.** We introduce now rescaled angular variables for the two back-to-back jets (left and right jet). For  $\theta_{\text{in}} \rightarrow 0$  the radiator is

$$r_{ab} = -2 \ln \frac{\theta_{\text{in}}}{2} - \frac{1}{2} \ln(1 - a^2) - \frac{1}{2} \ln(1 - b^2) , \quad \vec{a} = \frac{\theta_a}{\theta_{\text{in}}} \vec{n}_a , \quad \vec{b} = \frac{\pi - \theta_b}{\theta_{\text{in}}} \vec{n}_b . \quad (6.24)$$

This explicit  $\theta_{\text{in}}$  dependence implies that  $G_{ab}(\Delta)$  is given by  $\theta_{\text{in}}^{2\Delta}$  (the bremsstrahlung contribution) times a function of the rescaled variables  $\vec{a}, \vec{b}$ , whereas the same jet distribution depends only on the rescaled quantities.

The  $a$  and  $b$  contributions enter (6.24) independently. This is due to the fact that  $w_{ab}(k)$  splits into a sum of right and left pieces. As a consequence the evolution in the right and left regions develops independently and  $G_{ab}(\Delta)$  factorizes

$$G_{ab}(\Delta) \simeq \left( \frac{\theta_{\text{in}}}{2} \right)^{2\Delta} \cdot F_a^{\text{R}}(\Delta) \cdot F_b^{\text{L}}(\Delta) . \quad (6.25)$$

Here  $F_a^{\text{R}}$  and  $F_b^{\text{L}}$  satisfy the right and left evolutions and for the first we find

$$\partial_\Delta F_a^{\text{R}} = \frac{1}{2} \ln(1 - a^2) \cdot F_a^{\text{R}} + \int \frac{d^2 \vec{k}}{2\pi (\vec{a} - \vec{k})^2} [G_{ak}^{\text{RR}} F_k^{\text{R}} - F_a^{\text{R}}] , \quad (6.26)$$

where  $G_{ak}^{\text{RR}}$  is the distribution for  $a$  and  $k$  in the same (right) jet region discussed above. Proceeding as in subsection 6.2 we find the following asymptotic behaviour for the distribution with  $ab$  in opposite jet regions

$$G_{ab}(\Delta) \simeq e^{-\frac{\epsilon}{2}\Delta^2} \left( \frac{\theta_{\text{in}}^2 \hat{\lambda}(\vec{a}) \hat{\lambda}(\vec{b}) e^{-c'}}{2} \right)^\Delta \hat{f}(\vec{a}) \hat{f}(\vec{b}) , \quad (6.27)$$

with  $c'$  the integration constant given in (6.12) and  $\hat{f}$  an integration constant depending only on the rescaled variable. This expression shows that for small  $\theta_{\text{in}}$  the function  $f_{ab}(\theta_{\text{in}})$  in (6.19) factorizes and depends on the rescaled variables. The  $\theta_{\text{in}}$ -dependence is the one given by the bremsstrahlung contribution. The secondary branching contribution does not depend on  $\theta_{\text{in}}$  and is decreasing with  $\Delta$  with a Gaussian behaviour. For the physical  $e^+e^-$  distribution we set  $a^2 = b^2 = 0$ .

A generalization of this result is to the case where the two jets  $p_i p_j$  are not back-to-back but are set at an angle  $\theta_{ij}$ . The asymptotic behaviour is given by the expression (6.27) with  $\{2\}^{-\Delta}$  replaced by  $\{1 - \cos \theta_{ij}\}^{-\Delta}$  and with  $\theta_a$  the angle of  $a$  with respect to the jet  $p_i$  and  $\theta_b$  the angle of  $b$  with  $p_i$ . The physical distribution  $G_{p_i p_j}(\Delta)$  is again obtained by setting  $a^2 = b^2 = 0$ .

## 7. Discussion

We summarize here the essential physical points of our results on energy flow away from hard jets. The interjet distribution reduces to  $G_{p\bar{p}}(\Delta)$  in (3.7) for  $e^+e^-$ , while for DIS and hadron-hadron collisions it is given in terms of  $G_{p_i p_j}(\Delta)$ , see (A.5) and (A.11). These distributions depend on the geometry of  $\mathcal{C}_{\text{out}}$  and on the jet directions.

A characteristic of interjet observables is that the leading contribution to their distributions are SL, originating from soft emission at large angles. Collinear singularities here are subleading. The contribution from bremsstrahlung emission from the primary hard partons does not give the full SL structure. Indeed we find (see (4.9))

$$G_{p_i p_j}(\Delta) = e^{-R_{p_i p_j}^{(0)}(\Delta)} \cdot g_{p_i p_j}(\Delta) , \quad (7.1)$$

with  $R_{p_i p_j}^{(0)}(\Delta)$  the SL Sudakov radiator for emission into  $\mathcal{C}_{\text{out}}$ . The additional SL factor  $g_{p_i p_j}$  is generated by soft secondary emission, which can be described by successive colour singlet soft dipole emission. This implies that, in the present formulation, we work in the large  $N_c$  approximation. The soft secondary branching develops with

decreasing energy inside the unobserved jet region  $\mathcal{C}_{\text{in}}$  until a soft gluon enters  $\mathcal{C}_{\text{out}}$ . The emission is also effectively angular ordered.

At large  $\Delta$  the distribution  $G_{p_i p_j}(\Delta)$  decreases with a universal Gaussian behaviour, see equation (5.8), with a process-independent coefficient  $c$  that we have estimated to be  $c \approx 2.5$  with a 10% accuracy. Since the bremsstrahlung radiator is proportional to  $\Delta$  we see that the large  $\Delta$  behaviour is dominated by the soft secondary branching contribution  $g_{p_i p_j}(\Delta)$ .

The origin of the universal Gaussian behaviour in  $\Delta$  is a consequence of the structure of the branching. The secondary branching generating  $g_{p_i p_j}(\Delta)$  develops within a small cone  $\theta_{\text{crit}}(\Delta)$  around the hard primary partons  $p_i$  and  $p_j$ , which decreases exponentially for large  $\Delta$  according to (5.7), again governed by the universal coefficient  $c$ . It is the development of soft secondary branching in this peak region which generates the Gaussian behaviour in (5.8). At large  $\Delta$  the region within  $\theta_{\text{crit}}(\Delta)$  shrinks generating an empty buffer region first observed in [2]. For the case of figure 1 we have estimated that the asymptotic regime sets in around  $\Delta = 3$ . At this value the distribution is negligible away from the peak and approaches the asymptotic limit of figure 2.

Taking the jet region  $\mathcal{C}_{\text{in}}$  to be an arrangement of small cones centred on each hard jet leads to a universal secondary emission function  $g(\Delta)$  that depends neither on the size of the cones nor on the directions of the jets (see (5.10)).

The distribution  $G_{p_i p_j}(\Delta)$  is a function of  $E, E_{\text{out}}$  and the coupling  $\alpha_s$  through the quantity  $\Delta$  defined in (4.6). This involves an integral over the running coupling at low scales, and so acquires non-perturbative power corrections. These corrections can be estimated by the same method [14] used for the standard shape variables in  $e^+e^-$  and are expressed in term of a unique parameter  $\lambda^{\text{NP}}$  given by the integral over the running coupling in the low energy region. We obtain

$$\Delta \equiv \int_0^E \frac{d\omega}{\omega} \bar{\alpha}_s(\omega) [1 - e^{-\omega/E_{\text{out}}}] \simeq \int_{E_{\text{out}}}^E \frac{d\omega}{\omega} \bar{\alpha}_s(\omega) + N_c \frac{\lambda^{\text{NP}}}{2E_{\text{out}}}. \quad (7.2)$$

The non-perturbative parameter  $\lambda^{\text{NP}}$  (for the normalization used here see [15]) is measured both at LEP [16] and at HERA [17].

In hadron-hadron collisions one expects [1, 5, 12] additional large contributions to interjet observables coming from a soft underlying event generated by the incoming hadrons. We can write

$$E_{\text{out}} = \sum_{i \in \mathcal{C}_{\text{out}}} \omega_i + E_{\text{out}}^{\text{soft}}, \quad (7.3)$$

where the sum includes all partons produced in the hard process, and the quantity  $E_{\text{out}}^{\text{soft}}$  is the contribution of the soft underlying event. Assuming the underlying emission and hard emission factorize, the final answer will be given by the distribution

studied here with the replacement

$$\Delta(E, E_{\text{out}}) \rightarrow \Delta(E, E_{\text{out}} - E_{\text{out}}^{\text{soft}}). \quad (7.4)$$

Up to now in hadron-hadron collisions only the mean value of  $E_{\text{out}}$  has been investigated both theoretically and experimentally. One shows that the hard contribution, which can be reliably computed by fixed order QCD calculation<sup>6</sup>, does not fit the data [1, 4, 5] but requires a sizable  $E_{\text{out}}^{\text{soft}}$  contribution.

The resummed PT distribution here discussed provides a way to further study the underlying event, in particular its factorization properties and its size.

## Acknowledgements

We would like to thank Gavin Salam, Mrinal Dasgupta and Giulia Zanderighi for helpful discussions and suggestions.

---

<sup>6</sup>The PT calculation in [1] has been done only to  $\alpha_s^3$  order, now it is possible to perform the calculation at order  $\alpha_s^4$  [18] so that one can control the QCD scales.

## A. Interjet observables in DIS and hadron-hadron collisions

We introduce first the physical observables and then the QCD resummation.

### A.1 The observable

An example of an interjet distribution in DIS is given by

$$\Sigma_{\text{DIS}}(E_{\text{out}}) = \left\{ \sum_n \int \frac{d\sigma_n}{dx_B dQ^2} \right\}^{-1} \sum_n \int \frac{d\sigma_n}{dx_B dQ^2} \cdot \Theta \left( E_{\text{out}} - \sum_{h \in \mathcal{C}_{\text{out}}} \omega_h \right), \quad (\text{A.1})$$

with  $d\sigma_n/dx_B dQ^2$  the  $n$ -hadron distribution for fixed Bjorken variable  $x_B$  and  $Q^2$ . The events are dominated by the incoming and the outgoing hard jet. In the Breit frame the situation is similar to  $e^+e^-$  with both jets aligned along the beam direction. We may define the  $\mathcal{C}_{\text{out}}$  region by

$$-\eta_{\text{in}}^{(-)} < \ln \tan \frac{\theta_h}{2} < \eta_{\text{in}}^{(+)} . \quad (\text{A.2})$$

An example of an interjet distribution in hadron-hadron collisions with hard jets is

$$\Sigma_{\text{hh}}(E_{\text{out}}) = \left\{ \sum_n \int \frac{d\sigma_n}{d\eta dP_t} \right\}^{-1} \sum_n \int \frac{d\sigma_n}{d\eta dP_t} \cdot \Theta \left( E_{\text{out}} - \sum_{h \in \mathcal{C}_{\text{out}}} \omega_h \right), \quad (\text{A.3})$$

with  $d\sigma_n/d\eta dP_t$  the  $n$ -hadron distribution associated to the emission of a jet with rapidity  $\eta$  and transverse momentum  $P_t$ . The jet could be defined by a  $k_t$ -jet finding algorithm [19]. Here the event is dominated by the presence of an additional recoiling outgoing jet. The interjet region  $\mathcal{C}_{\text{out}}$  should be defined by avoiding the two incoming and the two outgoing hard jets. It is given for instance by fixing a region in the rapidity  $\eta_h$  and azimuthal angle  $\phi_h$  of emitted hadrons with respect to the triggered jet, see [4, 5].

The QCD resummation discussed for  $e^+e^-$  annihilation in section 3 can be generalized to the above processes due to the factorization of the parton process (see for instance [20]) as we shall discuss.

### A.2 QCD resummation: DIS case

To express the result for  $\Sigma_{\text{DIS}}(E_{\text{out}})$  we write the DIS cross section in the form

$$\frac{d\sigma}{dx_B dQ^2} = \int dx_1 \frac{d\sigma_{\gamma+p_1 \rightarrow p_2}(x_1, \mu)}{dx_1 dx_B dQ^2}, \quad \mu \sim Q, \quad (\text{A.4})$$

where  $d\sigma_{\gamma+p_1 \rightarrow p_2}(x_1, \mu)$  is the factorized parton distribution including the parton density function at the hard scale  $\mu \sim Q$  and the squared matrix element of the hard vertex  $\gamma^* + p_1 \rightarrow p_2$ . Here  $x_1$  is the momentum fraction of the hard parton  $p_1$  coming

into the hard vertex in the Breit frame. In the soft limit  $p_1$  and  $p_2$  correspond to the directions of the incoming and outgoing jets respectively.

By performing the same analysis as done in section 3 we obtain

$$\Sigma_{\text{DIS}}(E_{\text{out}}) = \left\{ \frac{d\sigma}{dx_B dQ^2} \right\}^{-1} \int dx_1 \frac{d\sigma_{\gamma+p_1 \rightarrow p_2}(x_1, \mu)}{dx_1 dx_B dQ^2} \cdot G_{p_1 p_2}(Q, E_{\text{out}}). \quad (\text{A.5})$$

The factorization scale remains at  $\mu$  since no observation is made in the collinear region. Here  $G_{p_1 p_2}(Q, E_{\text{out}})$  is the distribution introduced in (3.8) with  $p_1 p_2$  aligned, in the Breit frame, along the beam direction.

### A.3 QCD resummation: hadron-hadron case

The situation here is more involved since we have four jets (two outgoing and two incoming). There are various hard elementary processes

$$p_1 + p_2 \rightarrow p_3 + p_4, \quad (\text{A.6})$$

according to the nature ( $q, \bar{q}$  or  $g$ ) of the four involved partons. They are:

$$\begin{aligned} \text{A} \quad & q(p_1) + q'(p_2) \rightarrow q(p_3) + q'(p_4), \\ \text{B} \quad & q(p_1) + q(p_2) \rightarrow q(p_3) + q(p_4), \\ \text{C} \quad & q(p_1) + \bar{q}(p_2) \rightarrow g(p_3) + g(p_4), \\ \text{D} \quad & g(p_1) + g(p_2) \rightarrow g(p_3) + g(p_4), \end{aligned} \quad (\text{A.7})$$

together with those obtained by crossing transformations.

Energy flow in interjet regions for this process has been studied in [3] as far as the SL bremsstrahlung radiator piece. To construct the SL contribution from the soft secondary branching we need to represent the soft  $n$ -gluon emission in each of the hard processes (A.6) as a combination of colour singlet dipole emissions (3.3) from the four hard partons. The square amplitude for the emission in (A.6) of a single soft gluon  $k$  has been written in [21]. Taking the large  $N_c$  limit, this result can be expressed [22] as a sum of dipole emissions  $w_{ij}(k)$  from pairs  $p_i p_j$  of hard partons with the factorized structure

$$M_{f_1 f_2 f_3 f_4, k}^2 \rightarrow M_{f_1 f_2 f_3 f_4}^2 \cdot \sum_{\gamma} C_{f_1 f_2 f_3 f_4}^{(\gamma)} \sum_{\langle ij \rangle \in \gamma} \frac{\bar{\alpha}_s}{\omega_k^2} w_{ij}(k), \quad \sum_{\gamma} C_{f_1 f_2 f_3 f_4}^{(\gamma)} = 1, \quad (\text{A.8})$$

where  $M_{f_1 f_2 f_3 f_4}^2$  is the exact hard elementary  $2 \rightarrow 2$  distribution for the process (A.6) with  $f_i$  the type of parton  $p_i$ . The coefficients  $C_{f_1 f_2 f_3 f_4}^{(\gamma)}$  are functions of the kinematical invariants  $\hat{s} = (p_1 + p_2)^2$ ,  $\hat{t} = (p_1 - p_3)^2$ ,  $\hat{u} = (p_1 - p_4)^2$  and can be found in [22]. Here  $\gamma$  represents the set of all colour-connected partons in the specific hard process and the last sum is over all colour connected pairs  $ij$  in the set  $\gamma$ .

The simplest process is  $qq' \rightarrow qq'$  with only  $\langle f_1 f_4 \rangle$  and  $\langle f_2 f_3 \rangle$  colour connections. Here the coefficients are independent of the invariants and, from symmetry, we have

$$\sum_{\gamma} C_{qq'qq'}^{(\gamma)} \sum_{\langle ij \rangle \in \gamma} w_{ij}(k) = w_{14}(k) + w_{23}(k). \quad (\text{A.9})$$

The most complex process is  $gg \rightarrow gg$  for which all possible colour connections contribute.

The distribution for the emission in the hard process (A.6) of  $n$  additional soft gluons in the strongly energy ordered region is obtained by performing the analysis done in [7, 11] in the large  $N_c$  limit. Each additional soft gluon contributes to one of the hard dipole emissions as done in (3.3). This allows us to extend the analysis of section 3 and deduce the interjet  $E_{\text{out}}$  distribution in hadron-hadron collisions with a hard jet of rapidity  $\eta$  and transverse momentum  $P_t$ .

Consider the hadronic cross section for this process which we write in the form

$$\frac{d\sigma}{d\eta dP_t} = \sum_{\{f_i\}} \int dx_1 dx_2 \frac{d\sigma_{f_1 f_2 \rightarrow f_3 f_4}(x_1 x_2, \mu)}{dx_1 dx_2 d\eta dP_t}, \quad \mu \sim P_t, \quad (\text{A.10})$$

where  $d\sigma_{f_1 f_2 \rightarrow f_3 f_4}$  is the parton process integrand which includes parton density functions and hard parton distribution  $M_{f_1 f_2 f_3 f_4}^2$  for the elementary process (A.6). The normalized  $E_{\text{out}}$  distribution in a given interjet region  $\mathcal{C}_{\text{out}}$  is then given by

$$\begin{aligned} \Sigma_{\text{hh}}(E_{\text{out}}) &= \left\{ \frac{d\sigma}{d\eta dP_t} \right\}_{\{f_i\}}^{-1} \sum_{\{f_i\}} \int dx_1 dx_2 \frac{d\sigma_{f_1 f_2 \rightarrow f_3 f_4}(x_1 x_2, \mu)}{dx_1 dx_2 d\eta dP_t} \Sigma_{f_1 f_2 f_3 f_4}(P_t, E_{\text{out}}), \\ \Sigma_{f_1 f_2 f_3 f_4}(P_t, E_{\text{out}}) &= \sum_{\gamma} C_{f_1 f_2 f_3 f_4}^{(\gamma)} \prod_{\langle ij \rangle \in \gamma} G_{p_i p_j}(P_t, E_{\text{out}}), \end{aligned} \quad (\text{A.11})$$

where  $G_{p_i p_j}(P_t, E_{\text{out}})$  is the distribution introduced in (3.8) associated with the dipole  $p_i, p_j$ . In the soft limit we can take  $p_1 p_2$  in the direction of the two incoming hadrons and  $p_3 p_4$  in the direction of the two outgoing hard jets. We report the explicit form of  $\Sigma_{f_1 f_2 f_3 f_4}(P_t, E_{\text{out}})$  for the elementary processes in (A.7):

$$\begin{aligned} H^A \Sigma^A &= h^A(\hat{s}, \hat{t}, \hat{u}) G_{14} G_{23}, \\ H^B \Sigma^B &= h^B(\hat{s}, \hat{t}, \hat{u}) G_{14} G_{23} + h^B(\hat{s}, \hat{u}, \hat{t}) G_{13} G_{24}, \\ H^C \Sigma^C &= h^C(\hat{s}, \hat{t}, \hat{u}) G_{34} G_{13} G_{24} + h^C(\hat{s}, \hat{u}, \hat{t}) G_{34} G_{14} G_{23}, \\ H^D \Sigma^D &= h^D(\hat{s}, \hat{t}, \hat{u}) G_{12} G_{24} G_{43} G_{31} + h^D(\hat{s}, \hat{u}, \hat{t}) G_{12} G_{23} G_{34} G_{41} \\ &\quad + h^D(\hat{u}, \hat{t}, \hat{s}) G_{14} G_{42} G_{23} G_{31}, \end{aligned} \quad (\text{A.12})$$



$$\begin{aligned}
h^A(s, t, u) &= g^4 \frac{C_F}{N_c} \left( \frac{s^2+u^2}{t^2} \right) \\
h^B(s, t, u) &= h^A(s, t, u) + 2g^4 \frac{C_F}{N_c^2} \frac{s}{t} \\
h^C(s, t, u) &= g^4 C_F \frac{u}{t} \left( \frac{t^2+u^2}{s^2} - \frac{1}{N_c^2} \right) \\
h^D(s, t, u) &= 2g^4 \left( \frac{N_c^2}{N_c^2-1} \right) \left( 1 - \frac{tu}{s^2} - \frac{su}{t^2} + \frac{u^2}{st} \right)
\end{aligned}$$

**Table 1:** The functions  $h^{(A,B,C,D)}$  taken from Ref. [22].

with  $G_{ij} = G_{p_i p_j}(P_t, E_{\text{out}})$  and the functions  $h^{(A,B,C,D)}$  given in table 1. Here

$$\begin{aligned}
H^A &= h^A(\hat{s}, \hat{t}, \hat{u}), \\
H^B &= h^B(\hat{s}, \hat{t}, \hat{u}) + h^B(\hat{s}, \hat{u}, \hat{t}), \\
H^C &= h^C(\hat{s}, \hat{t}, \hat{u}) + h^C(\hat{s}, \hat{u}, \hat{t}), \\
H^D &= h^D(\hat{s}, \hat{t}, \hat{u}) + h^D(\hat{s}, \hat{u}, \hat{t}) + h^D(\hat{u}, \hat{t}, \hat{s}),
\end{aligned} \tag{A.13}$$

are the square amplitudes for the  $2 \rightarrow 2$  elementary processes (A.7).

The structure in (A.12) in terms of the factorized distributions  $G_{ij}$  is derived from eq. 66 of Ref. [22] in which we have identified  $2C_F$  with  $C_A$  since we work in the large  $N_c$  limit. Going beyond the large  $N_c$  approximation requires the analysis of colour interference between different hard partons. At the moment this can be done only for the bremsstrahlung contribution, elegantly computed in [3], see also [23].

In conclusion, for all considered hard processes, the interjet distributions are described by the universal function  $G_{p_i p_j}(E, E_{\text{out}})$  which depends on the two hard jet directions  $p_i$  and  $p_j$  (incoming or outgoing) and on the interjet region  $\mathcal{C}_{\text{out}}$ .

## B. Theorem: $0 \leq G_{ab}(\Delta) \leq 1$

In this appendix we show that the solution of the differential equation (4.8) with the given boundary condition is bounded below and above by 0 and 1. Thus our distribution is physically meaningful.

Proof:

1.  $G_{ab}(\Delta)$  is a continuous function of  $\Delta$  and of  $a$  and  $b$ .
2.  $G_{ab}(0) = 1 \forall a, b$ .
3. If  $a = b$  then  $G_{ab}(\Delta) = 1 \forall \Delta$ .
4. Suppose  $\exists a', b'$  and  $\Delta'$  with  $G_{a'b'}(\Delta') > 1$ . Then by continuity  $\exists a'', b''$  and  $\Delta''$  with  $0 \leq \Delta'' < \Delta'$ ,  $G_{ab}(\Delta'') \leq 1 \forall a, b$ , and  $a'' \neq b''$ ,  $G_{a''b''}(\Delta'') = 1$ ,  $\partial_\Delta G_{a''b''}(\Delta'') \geq 0$ .

5. But by (4.8) we have  $\partial_\Delta G_{a''b''}(\Delta'') < 0$  which gives a contradiction. Therefore  $G_{ab}(\Delta) \leq 1 \forall a, b, \Delta$ .
6. Suppose now  $\exists a', b'$  and  $\Delta'$  with  $G_{a'b'}(\Delta') < 0$ . Then by continuity  $\exists a'', b''$  and  $\Delta''$  with  $0 \leq \Delta'' < \Delta'$ ,  $G_{ab}(\Delta'') \geq 0 \forall a, b$ , and  $a'' \neq b''$ ,  $G_{a''b''}(\Delta'') = 0$ ,  $\partial_\Delta G_{a''b''}(\Delta'') \leq 0$ .
7. But by (4.8) we have  $\partial_\Delta G_{a''b''}(\Delta'') > 0$  which gives a contradiction. Therefore  $G_{ab}(\Delta) \geq 0 \forall a, b, \Delta$ .

### C. Iterative solution

Here we calculate the first term  $R_{p\bar{p}}^{(1)}(\Delta)$  in the iterative solution described in section 5.1. First we have that for any  $a, b$  the bremsstrahlung emission is given by

$$r_{ab} = \frac{s_a}{2} \ln \frac{\cos \theta_a + \cos \theta_{\text{in}}}{\cos \theta_a - \cos \theta_{\text{in}}} + \frac{s_b}{2} \ln \frac{\cos \theta_b + \cos \theta_{\text{in}}}{\cos \theta_b - \cos \theta_{\text{in}}} + \frac{s_a + s_b}{4} \times \ln \frac{(1 + \cos^2 \theta_{\text{in}})(1 + \cos \theta_a \cos \theta_b) - 2 \cos \theta_{\text{in}} (\cos \theta_a + \cos \theta_b) - \sin^2 \theta_{\text{in}} \sin \theta_a \sin \theta_b \cos \phi_{ab}}{(1 + \cos^2 \theta_{\text{in}})(1 + \cos \theta_a \cos \theta_b) + 2 \cos \theta_{\text{in}} (\cos \theta_a + \cos \theta_b) - \sin^2 \theta_{\text{in}} \sin \theta_a \sin \theta_b \cos \phi_{ab}}, \quad (\text{C.1})$$

where  $s_k = 1$  for  $\cos \theta_k > 0$  and  $s_k = -1$  for  $\cos \theta_k < 0$ . Therefore we obtain  $R_{ab}^{(0)}$  in the following cases

$$\begin{aligned} R_{p\bar{p}}^{(0)}(\Delta) &= \Delta \cdot \ln \frac{1 + \cos \theta_{\text{in}}}{1 - \cos \theta_{\text{in}}}, \\ R_{p\bar{k}}^{(0)}(\Delta) &= \Delta \cdot \frac{s_k}{2} \ln \frac{(1 - \cos \theta_{\text{in}})(\cos \theta_k + \cos \theta_{\text{in}})}{(1 + \cos \theta_{\text{in}})(\cos \theta_k - \cos \theta_{\text{in}})}, \\ R_{k\bar{p}}^{(0)}(\Delta) &= \Delta \cdot \frac{s_k}{2} \ln \frac{(1 + \cos \theta_{\text{in}})(\cos \theta_k + \cos \theta_{\text{in}})}{(1 - \cos \theta_{\text{in}})(\cos \theta_k - \cos \theta_{\text{in}})}. \end{aligned} \quad (\text{C.2})$$

Now using the definition (5.4) we explicitly calculate

$$R_{p\bar{p}}^{(1)}(\Delta) = \int_0^\Delta d\Delta' \int_{\mathcal{C}_{\text{in}}} \frac{d^2 \Omega_k}{4\pi} w_{p\bar{p}}(k) \left[ 1 - U_{p\bar{p}k}^{(0)}(\Delta') \right], \quad (\text{C.3})$$

where

$$U_{p\bar{p}k}^{(0)}(\Delta) = \left( \frac{|\cos \theta_k| - \cos \theta_{\text{in}}}{|\cos \theta_k| + \cos \theta_{\text{in}}} \right)^\Delta \left( \frac{1 + \cos \theta_{\text{in}}}{1 - \cos \theta_{\text{in}}} \right)^\Delta. \quad (\text{C.4})$$

For large  $\Delta$  the integrand  $[1 - U_{p\bar{p}k}^{(0)}(\Delta)]$  forces  $k$  to stay away from the thrust axis by an small angle of order  $\Delta^{-1}$ . Changing integration variables we have

$$R_{p\bar{p}}^{(1)}(\Delta) = \int_0^\Delta d\Delta' \int_0^1 dx \left( \frac{1 - x^{\Delta'}}{1 - x} - \frac{1 - x^{\Delta'}}{\cot^4 \frac{\theta_{\text{in}}}{2} - x} \right). \quad (\text{C.5})$$

At small  $\Delta$  this gives the result (5.5), while at large  $\Delta$  we obtain (5.6).

## References

- [1] G. Marchesini and B.R. Webber, *Phys. Rev.* **D 38** (1988) 3419.
- [2] M. Dasgupta and G. P. Salam, *J. High Energy Phys.* **03** (2002) 017 [hep-ph/0203009].
- [3] C. F. Berger, T. Kucs and G. Sterman, *Phys. Rev.* **D 65** (2002) 094031 [hep-ph/0110004].
- [4] UA1 Collaboration, C. Albajar et al. *Nucl. Phys.* **B 309** (1988) 405.
- [5] J. Huston and V. Tano, in “The QCD and standard model working group: Summary report”, hep-ph/0005114;  
R. D. Field [CDF Collaboration], hep-ph/0201192;  
W. Giele *et al.*, “The QCD/SM working group: Summary report”, hep-ph/0204316.
- [6] A.H. Mueller, *Phys. Lett.* **B 104** (1981) 161;  
B. I. Ermolaev and V. S. Fadin, *JETP Lett.* **33**, 269 (1981) [*Pisma Zh. Eksp. Teor. Fiz.* **33**, 285 (1981)];  
A. Bassetto, M. Ciafaloni, G. Marchesini and A. H. Mueller, *Nucl. Phys.* **B 207** (1982) 189;  
Y. L. Dokshitzer, V. A. Khoze, A. H. Mueller and S. I. Troyan, *Gif-sur-Yvette, France: Ed. Frontieres (1991) 274 p. (Basics of perturbative QCD)*.
- [7] A. Bassetto, M. Ciafaloni and G. Marchesini, *Phys. Rep.* **100** (1983) 201.
- [8] S. Catani, L. Trentadue, G. Turnock and B.R. Webber, *Nucl. Phys.* **B 407** (1993) 3;  
S. Catani and B.R. Webber, *Phys. Lett.* **B 427** (1998) 377 [hep-ph/9801350];  
Yu.L. Dokshitzer, A. Lucenti, G. Marchesini and G.P. Salam, *J. High Energy Phys.* **01** (1998) 011 [hep-ph/9801324].
- [9] L.N. Lipatov, *Sov. J. Nucl. Phys.* **20** (1975) 94;  
V.N. Gribov and L.N. Lipatov, *Sov. J. Nucl. Phys.* **15** (1972) 438;  
G. Altarelli and G. Parisi, *Nucl. Phys.* **B 126** (1977) 298;  
Yu.L. Dokshitzer *Sov. Phys. JETP* **46** (1977) 641.
- [10] M. Dasgupta and G. P. Salam, *Phys. Lett.* **B 512** (2001) 323 [hep-ph/0104277].
- [11] F. Fiorani, G. Marchesini and L. Reina, *Nucl. Phys.* **B 309** (1988) 439.
- [12] G. Corcella, I.G. Knowles, G. Marchesini, S. Moretti, K. Odagiri, P. Richardson, M.H. Seymour, B.R. Webber, *J. High Energy Phys.* **01** (2001) 010 [hep-ph/0011363];  
T. Sjostrand, *Comput. Phys. Commun.* **82** (1994) 74;  
L. Lonnblad, *Comput. Phys. Commun.* **71** (1992) 15.
- [13] S. Catani, G. Marchesini and B.R. Webber, *Nucl. Phys.* **B 349** (1991) 635.

- [14] B.R. Webber, *Phys. Lett.* **B 339** (1994) 148 [hep-ph/9408222];  
M. Beneke and V.M. Braun, *Nucl. Phys.* **B 454** (1995) 253 [hep-ph/9506452];  
Yu.L. Dokshitzer and B.R. Webber, *Phys. Lett.* **B 352** (1995) 451 [hep-ph/9504219];  
R. Akhoury and V.I. Zakharov, *Phys. Lett.* **B 357** (1995) 646 [hep-ph/9504248]; *Nucl. Phys.* **B 465** (1996) 295 [hep-ph/9507253];  
G.P. Korchemsky and G. Sterman, *Nucl. Phys.* **B 437** (1995) 415 [hep-ph/9411211];  
Yu.L. Dokshitzer, V.A. Khoze and S.I. Troyan, *Phys. Rev.* **D 53** (1996) 89 [hep-ph/9506425];  
P. Nason and M.H. Seymour, *Nucl. Phys.* **B 454** (1995) 291 [hep-ph/9506317];  
Yu.L. Dokshitzer, G. Marchesini and B.R. Webber, *Nucl. Phys.* **B 469** (1996) 93 [hep-ph/9512336];  
M. Beneke, *Phys. Rep.* **317** (1999) 1 [hep-ph/9807443].
- [15] A. Banfi, G. Marchesini and G. Smye, *J. High Energy Phys.* **04** (2002) 024 [hep-ph/0203150].
- [16] P. A. Movilla Fernandez, O. Biebel, S. Bethke, paper contributed to the EPS-HEP99 conference in Tampere, Finland, hep-ex/9906033.  
H. Stenzel, MPI-PHE-99-09 *Prepared for 34th Rencontres de Moriond: “QCD and Hadronic interactions”*, Les Arcs, France, 20-27 Mar 1999;  
ALEPH Collaboration, “QCD Measurements in e+e- Annihilations at Centre-of-Mass Energies between 189 and 202 GeV”, ALEPH 2000-044 CONF 2000-027;  
P. Abreu *et al.* (DELPHI Collaboration), *Phys. Lett.* **B 456** (1999) 322;  
DELPHI Collaboration, “The Running of the Strong Coupling and a Study of Power Corrections to Hadronic Event Shapes with the DELPHI Detector at LEP”, DELPHI 2000-116 CONF 415, July 2000.  
M. Acciarri *et al.* (L3 Collaboration), *Phys. Lett.* **B 489** (2000) 65 [hep-ex/0005045].
- [17] C. Adloff *et al.* [H1 Collaboration], *Eur. Phys. J.* **C 14** (2000) 255, erratum *ibid.* **C18** (2000) 417 [hep-ex/9912052];  
G. J. McCance [H1 collaboration], hep-ex/0008009.
- [18] Z. Bern , L.J. Dixon, and D.A. Kosower, *Phys. Rev. Lett.* **70** (1993) 2677 [hep-ph/9302280]; *Nucl. Phys.* **B 437** (1995) 259 [hep-ph/9409393];  
Z. Kunszt , A. Signer, and Z. Trócsányi, *Phys. Lett.* **B 336** (1994) 529 [hep-ph/9405386];  
J.G.M. Kuijf , Ph.D. thesis, Universiteit Leiden, 1991;  
J.F. Gunion and Z. Kunszt, *Phys. Lett.* **B 159** (1985) 167; *Phys. Lett.* **B 176** (1986) 477; *Phys. Lett.* **B 176** (1986) 163;  
Z. Nagy, *Phys. Rev. Lett.* **88** (2002) 122003 [hep-ph/0110315].
- [19] S. Catani, Y. L. Dokshitzer and B. R. Webber, *Phys. Lett.* **B 285** (1992) 291;  
S. Catani, Y. L. Dokshitzer, M. H. Seymour and B. R. Webber, *Nucl. Phys.* **B 406** (1993) 187.

- [20] J. C. Collins, D. E. Soper and G. Sterman, *Nucl. Phys.* **B 26** (1985) 104;  
G. T. Bodwin, *Phys. Rev.* **D 31** (1985) 2616, erratum *ibid.* **D34** (1986) 3932.
- [21] R. K. Ellis, G. Marchesini and B. R. Webber, *Nucl. Phys.* **B 286** (1987) 643, erratum  
*ibid.* **B294** (1987) 1180.
- [22] G. Marchesini and B. R. Webber, *Nucl. Phys.* **B 310** (1988) 461,
- [23] N. Kidonakis and G. Sterman, *Nucl. Phys.* **B 505** (1997) 321 [hep-ph/9705234];  
N. Kidonakis, G. Oderda and G. Sterman, *Nucl. Phys.* **B 531** (1998) 365 [hep-  
ph/9803241].